ISSN: 2352-9520

OpenNano

Cutting edge research in nanopharmaceutics & nanopharmacology

OpenNano 11 (2023) 100143

Contents lists available at ScienceDirect

OpenNano

journal homepage: www.elsevier.com/locate/onano

Cytotoxicity of magnetite nanoparticles deposited in sodium chloride matrix and their functionalized analogues in erythrocytes

Stanislav Lytvyn [a,1,*], Elena Vazhnichaya [b,2], Yurii Kurapov [a], Oleksandr Semaka [b], Lyubov Babijchuk [c,3], Pavlo Zubov [c,3]

[a] *Laboratory of Electron Beam Nanotechnology of Inorganic Materials for Medicine, E. O. Paton Electric Welding Institute of the National Academy of Sciences of Ukraine, 11, Kazymyr Malevych Street, Kyiv, 03150, Ukraine*

[b] *Department of Pharmacology, Clinical Pharmacology and Pharmacy, Poltava State Medical University, 23, Shevchenko Street, Poltava, 36011, Ukraine*

[c] *Department of Cryocytology, Institute for Problems of Cryobiology and Cryomedicine of the National Academy of Sciences of Ukraine, 23, Pereyaslavska Street, Kharkiv, 61016, Ukraine*

ARTICLE INFO

Keywords:
Magnetite ligand-free nanoparticles
Electron beam physical vapor deposition
Functionalization of nanoparticles
Cytotoxicity
Hemolysis
Erythrocyte shape, Membrane symmetry

ABSTRACT

The synthesis of covered nanoparticles provides new properties to the materials for biomedical applications. This fully applies to iron oxide nanoparticles. The research aim was to study features of the magnetite nanoparticles synthesized by electron beam technology as well as to investigate their functionalization and cytotoxicity. Nanoparticle characteristics were determined by standard methods. Cytotoxiciy of nanoparticles was studied using erythrocyte model. It was shown that the original magnetite nanoparticles in the sodium chloride matrix can be functionalized with polyvinylpyrrolidone and ethylmethylhydroxypyridine succinate, an antioxidant. All investigated nanoparticles were non-toxic for erythrocytes at concentrations up to 100 μg Fe/ml. At 100-200 μg Fe/ml, they increased the amount of cells expressing phosphatidylserine on the outer membrane, the count of pathological forms of erythrocytes and hemolysis. These phenomena were less pronounced if the nanosystem included the antioxidant. Therefore, magnetite nanoparticles can be obtained by electron beam technology and functionalized to form non-toxic nanosystems.

1. Background

The synthesis of varied nanoparticles (NPs) provides additional functional properties to the obtained materials [1]. This fully applies to NPs of metals and their oxides [2], in particular magnetic oxides based on physical methods of fabrication [3].

Abbreviations: D, Hydrodynamic diameter; DLS, Dynamic light scattering; EB PVD, Electron beam physical vapor deposition; EMHPS, Ethylmethylhydroxypyrydine succinate; Fe, Iron; Fe_3O_4, Magnetite, iron (II, III) oxide; NaCl, Sodium chloride; NP(s), Nanoparticle(s); pH, Hydrogen index; PVP, Polyvinylpyrrolidone; TEM, Transmission electron microscopy; XRD, X-ray diffraction.

* Corresponding author: Stanislav Lytvyn Tel: +38 (044) 205 2286 Fax: +38 (044) 200 6855

E-mail addresses: office@paton.kiev.ua, lytvynse@hotmail.com (S. Lytvyn), pharmacology@pdmu.edu.ua (E. Vazhnichaya), cryo.ua@gmail.com (L. Babijchuk), cryo.in.ua@gmail.com (P. Zubov).

[1] +38 (044) 206 1787

[2] +38 (0532) 562 059

[3] +38 (057) 373 4143, +38 (057) 373 8807, ,

https://doi.org/10.1016/j.onano.2023.100143
Received 25 December 2022; Received in revised form 9 March 2023; Accepted 16 March 2023
Available online 17 March 2023

NPs of magnetite (Fe_3O_4) have attracted the attention of researchers from the point of view of the biomedical applications. This is due to their common properties, such as biocompatibility [4], biodegradation [5], magnetic behavior [6] and the presence of the iron (Fe), which can be included in the normal metabolism of this element [7].

They are biocompatible because magnetite NPs demonstrate the ability to perform with an appropriate host response in specific situations [8]. These situations are diagnosis, treatment of the cancer or combating the iron deficiency for which some iron oxide NPs have already been approved for [9,10]. Other promising fields of their application include catalysis, environmental remediation, and electronics [11–13].

The factor that limits the use of newly created magnetite NPs is their potential toxicity, so toxicological studies are widely conducted [14]. Safety assessment of magnetite NPs on cell lines is a simple and inexpensive *in vitro* method [15,16]. The most widely used options for analyzing the viability, proliferation, and differentiation of cells under the influence of NPs are optical, electron, and atomic force microscopy [17]. Analysis of gene expression, proteomics, and metabolomics are new methods that facilitate the study of the magnetite NPs cytotoxicity [18,19]. Studying the cell in all these parameters is valuable for assessing the interaction between magnetic NPs and the cell, however, research results vary widely and are often contradictory.

It is believed that the toxicity of magnetite NPs relates to the concentration, exposure period, surface modification, size, and shape [20–22].

In particular, the dependence of toxic effects on the nature of NPs was demonstrated in a study where uncoated magnetite NPs, sodium oleate-coated NPs, and silicon dioxide NPs were used to assess toxicity parameters on the placental barrier cell model [23]. The results showed that cytotoxicity of magnetite NPs was more obvious and occurred at lower doses and shorter exposure compared to silica particles.

In another work, uncoated magnetite NPs were used to treat the NRK-52E cell line. Using comparative proteomics, it was shown that such NPs mobilized cellular protection to eliminate apoptosis [24]. The influence of the surface modification on the cytotoxicity of magnetite NPs was confirmed in a study where uncoated magnetite NPs (hydrophilic) and NPs coated with n-octyltriethoxysilane (hydrophobic) were tested on PC12 and ReNcell VM cells. For both cell lines, the hydrophobic coating weakened the cytotoxic effects [25]. Similarly, testing cationic magnetite NPs without coating, magnetite NPs functionalized with starch or dextran, and anionic maghemite NPs on PC12 rat pheochromocytoma cells showed that different types of NPs interact differently with the cells [26]. Uncoated magnetite NPs were on the outer surface of cells and did not show a cytotoxic effect at low concentrations. Magnetite NPs with starch or dextran formed aggregates and reduced cell viability. But maghemite NPs demonstrated penetration into cells without a cytotoxic effect at any studied concentrations.

The toxicity of magnetite NPs for cells depends not only on the presence of coating, but also by its characteristics, which emphasizes the importance of chemical design in the construction of magnetic NPs [27]. For example, the cytotoxicity of NPs with a short polymeric chain in the coating was much higher compared to long chains [28].

Most authors agree that up to a certain concentration of magnetite NPs, cytotoxicity is not detected [26,29,30]. In particular, dimercaptosuccinic acid-coated magnetite NPs had no significant effect on the viability, oxidative stress, cell cycle, or apoptosis of non-parenchymal hepatocytes at a concentration of 0.5 mg/ml [31].

In some cases, the toxicity of magnetite NPs was studied using blood cells. It was shown that these NPs do not cause damage of blood cells when incubated at +20°C for 2 h [32]. It was also described that iron oxide NPs coated with dextran did not show any toxic effect when interacting with human monocytes and macrophages at a concentration of 1 mg/ml [33]. At the same time, according to other data, magnetite NPs stabilized by citric acid contributed to the release of significantly more hemoglobin from erythrocytes than in the control and a hemolytic effect was dose-dependent [34].

The ambiguity of research results on the cytotoxicity of magnetite NPs and its dependence on numerous factors justify the need to determine the toxicity parameters in each case of the fabrication of new iron oxide NPs that have prospects for biomedical application. *In vitro* methods are available, relatively cheap and acceptable from the point of view of bioethics [35]. There is no single protocol for determining the NPs toxicity, and preference is given to the assessment of cytotoxicity.

As mentioned above, different cells serve model systems for determination of the NPs cytotoxycity, and erythrocyte model attract our attention because it was shown that eryptosis indices may be highly informative in the evaluation of magnetite NPs cytotoxicity, no worse than viability tests in cell cultures [36]. In addition, the results of cytotoxicity in relation to erythrocytes can be extrapolated to processes in the circulatory bed *in vivo* [36].

We use this approach to study the cytotoxicity for erythrocytes of magnetite NPs obtained by electron beam technology and functionalized with sodium chloride (NaCl) or with it together with ethylmethylhydroxypyridine succinate (EMHPS), polyvinylpyrrolidone (PVP), and both of these substances simultaneously. EMHPS was selected for NPs surface modification as potent synthetic antioxidant [37]. It is known as a drug with the non-patented international name "Mexidol", which is characterized by a wide safety margin and is widely the use in Ukraine for neurological and cardiological diseases [38]. For NPs functionalization, it has never been used before. Low molecular weight PVP is a water-soluble polymeric substance, an ingredient of the infusion colloidal solution "Hemodez-N", which is approved for clinical use in Ukraine [39]. PVP is also known as coating agent for iron oxide NPs [40,41]. It was assumed that the combination of both mentioned substances can ensure the stability of NPs, enhance the effect of nano-iron on hematopoiesis, and reduce the potential generation of reactive oxygen species to improve safety of this material.

2. Methods

2.1. Synthesis of magnetite nanoparticles

For the synthesis of ligand-free NPs, the method of electron beam simultaneous evaporation of iron and NaCl in vacuum through their liquid bath with physical vapor deposition (EB PVD) of mixed vapor streams on a water-cooled substrate was chosen [42]. Iron NPs in the porous NaCl matrix after opening the vacuum chamber were oxidized in air to magnetite. The starting iron ingot was obtained by double electron beam refining of armco-iron and had the shape of a cylinder. Purity of the starting iron was 99.9%. Block of NaCl was obtained by pressing salt of the highest grade.

2.2. Identification of original nanoparticles

The size and phase composition of NPs were confirmed by the transmission electron microscopy (TEM) and X-ray diffraction (XRD) analysis. TEM studies were performed on fresh condensate fracture and on samples after repeated washing of NPs in the condensate from salt in distilled water. The study took place at a transmission electron microscope HITACHI H-800 (Japan) at an accelerating voltage of 100 kV.

XRD analysis of finely ground condensate of NPs was carried out at a DRON-UM1 diffractometer with cobalt (Co K_α) radiation and a graphite monochromator in the reflected beam in the angle range of 10-85 degrees. The average crystallite size was estimated according to the Scherrer equation. Semi-quantitative phase analysis was performed using Match!

2.3. Functionalization of magnetite nanoparticles

We used a condensate of magnetite NPs deposited in NaCl matrix that, in fact, is *in situ* functionalization with the formation of Fe_3O_4@NaCl NPs. To obtain other NPs, additional functionalization of Fe_3O_4@NaCl NPs after the synthesis was carried out with EMHPS and (or) PVP in a liquid medium.

The substance of EMHPS was obtained from the manufacturer (NVF LLC Microhim, Ukraine). To functionalize Fe_3O_4@NaCl NPs, this agent was dissolved together with the NPs condensate in deionized water in the ratio of 1 mg of condensate/20 mg of EMHPS/1 ml of water for 2 h at +60°C and constant shaking.

PVP (8000±2000 D) was obtained from Novofarm-Biosyntez LLC (Ukraine). 3% solution of PVP (w/v) was prepared and powdered condensate of Fe_3O_4@NaCl was dissolved in it under the conditions described above. The ratio of condensate and PVP was 1 mg/30 mg in 1 ml of solution.

When functionalizing Fe_3O_4@NaCl simultaneously with EMHPS and PVP, the condensate of the NPs and EMHPS were dissolved in the 3% solution of PVP under the same conditions and ratio of ingredients as in the previous cases.

This made it possible to compare the effects of four types of functionalized magnetite NPs: Fe_3O_4@NaCl, Fe_3O_4@NaCl@EMHPS, Fe_3O_4@NaCl@PVP, Fe_3O_4@NaCl@EMHPS@PVP, hereinafter referred to as nanosystems 1-4, respectively. The working concentrations of these nanosystems were obtained by introducing the appropriate amount of basic solutions into the model media on the basis that 1 mg of the condensate contains 290 μg Fe.

2.4. Determination of the nanoparticles size distribution in solutions of nanosystems 1-4

After functionalization, the hydrodynamic diameter (D) of NPs in nanosystems 1-4 was determined by the dynamic light scattering (DLS) method [43]. The obtained results were processed in the program PCS Size Mode v.1.61 in the Contin approximation. Number and volume particle size distributions were obtained from three consecutive measurements. The research was carried out at a laser correlation spectrometer Zeta Sizer-3 (Malvern Instruments Co. Ltd., UK).

2.5. The method of erythrocytes obtaining

The experiments were performed on the blood of 25 intact albino rats, obtained by puncture of the heart according to the generally accepted method [44], which did not cause objections of the Bioethics Commission of the Poltava State Medical University. Blood samples were stabilized with EDTA. Erythrocytes, washed twice with sterile isotonic NaCl solution, were suspended in the isotonic NaCl solution, buffered with the phosphate buffer to pH=7.4, in a ratio corresponding to hematocrit. Each erythrocyte suspension was prepared from the blood of one rat. For incubation with NPs to 0.310, 0.655, 0.966, 0.983 and 0.997 ml of erythrocyte suspension, respectively, 0.690, 0.345, 0.034, 0.017 and 0.003 ml of the basic solution of each type of NPs were added. Basic solution contained 1 mg of Fe_3O_4@NaCl per 1 ml (beside coating agents when studying nanosystrms 2-4). This formed a series of samples with concentrations of 200, 100, 10, 5 and 1 μg Fe/ml. Suspensions without NPs served as controls.

2.6. Study of the pathology of erythrocyte shape

Experimental and control suspensions were incubated for 24 h at +20°C. After that, they were centrifuged for 5 min at 1000 rpm. From the sediment, smears were made on glass slides, fixed, stained according to Pappenheim and used to count erythrocytes with the shape pathology [45]. Light microscopy was performed under a microscope MICROmed XS-3320 (China). In the testing of each type of

NPs for each tested concentration, there were 5 observations.

2.7. Study of erythrocyte hemolysis

To determine the effect of the studied NPs on hemolysis, erythrocytes were incubated with nanosystems 1-4 at concentrations 1-200 μg Fe/ml for 24 h at +20°C. Erythrocytes, incubated with deionized water and isotonic NaCl solution, were used as positive and negative controls, respectively. After centrifugation at 1000 rpm for 3 min, the supernatants were collected for spectrophotometry at spectrophotometer Ulab-102 (Ulab COMPANY: LLC Chemlaboreaktiv, China). The optical density was analyzed at 570 nm and the percentage of hemolysis was calculated [36]. In the testing of each type of NPs for each concentration, there were 5 observations.

2.8. Determination of annexin V binding

The changes of erythrocyte membrane asymmetry were studied in suspensions prepared as described above. The concentration of NPs was 100 μg Fe/ml. Incubation lasted 24 h at +20°C. The degree of asymmetry of the erythrocyte membrane was assessed by the binding of annexin V to phosphatidylserine on the outer surface of the membrane [46]. The BD Annexin V-FITC detection KIT I kit was used in accordance with the Annexin V-FITC staining protocol. The samples were analyzed at a flow cytometer FACSCalibur (Becton Dickinson, USA). The results of measurements were evaluated using the software company BD - CELLQuest Pro. Every group contained 3 samples.

2.9. Statistical analysis

All data of biomedical experiments were expressed as mean M ± m (the error of the mean). The results were analyzed using Statistica for Windows v.6.0. p-value < 0.05 was considered statistically significant.

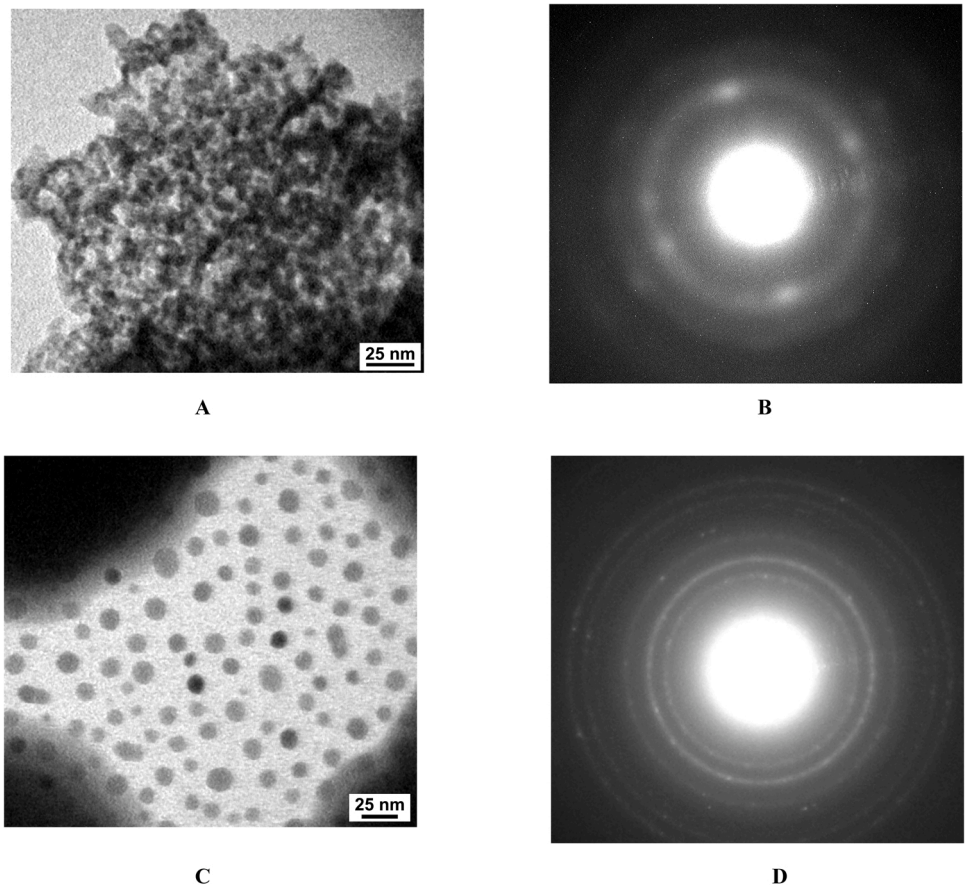

Fig. 1. TEM images (**a, c**) and electron diffraction pattern (**b, d**) of the initial 29 wt% Fe-NaCl condensates (**a, b**) and after rinsed in distilled water from salt (**c, d**).

3. Results

3.1. Characteristics of nanoparticles condensate obtained by EB PVD

The results of a TEM study were shown in Fig. 1. As can be seen from Fig. 1a, on a salt background iron NPs did not have a clear image. This was due to the instability of the image under the influence of the electron beam of the microscope on the loose structure of the NaCl matrix. The fact is that for the synthesis of iron NPs, the ratio of the intensities of NaCl and iron vapor streams during electron beam deposition from two sources should be at least 5:1. Then, due to the shadow effect of the iron metal particles, a porous structure of NaCl is formed, which does not have a single crystal lattice, is highly defective and inhomogeneous. This was confirmed by the diffraction pattern of Fig. 1b, where clear reflections from salt single crystals were observed against the background of solid lines from amorphous salt. The lines from iron were difficult to identify due to their overlap with the salt line and the low content. To identify the presence of the iron in the condensate, the salt was washed in a large amount of water and the dried sediment was examined. In this way, a clear image of NPs (Fig. 1c) and a diffractogram of only magnetite (Fig. 1d) were obtained.

TEM image analysis of 308 washed magnetite NPs (Fig. 1c, Fig. 2) gave an average size of 14.7 nm with a particle size range of 4.7–31.9 nm.

XRD analysis confirmed the size and phase composition of both the Fe-NaCl condensate and the salt-washed powder. With a significant content of iron in the condensate, NPs of large sizes did not have time to completely oxidize to magnetite, so XRD analysis along with magnetite recorded the remains of the pure Fe phase. However, during further crushing of the condensate and washing it from salt, complete oxidation of iron to magnetite occurred. Thus, the main studies were performed on the condensates with a size of NPs of 5-32 nm and a phase composition of Fe_3O_4.

3.2. DLS characteristics of nanosystems 1-4

Number (Fig. 3a, c, e, g) and volume (Fig. 3b, d, f, h) particle size distribution was obtained from three consecutive measurements.

Nanosystem 1 when studying the particle size distribution by volume (Fig. 3b) showed two fractions. The first fraction was formed by particles with an average size of 22 nm and a volume fraction of 54% (Fig. 3). Their number was 99.9% (Fig. 3a). The second fraction had a maximum at 870 nm (Fig. 3b). The number of particles of this fraction was 0.1% (Fig. 3a), and the volume share was 46%.

In nanosystem 2, two fractions of particle distribution were revealed (Fig. 3c, d). The specific gravity of the first of them was 0.1% (Fig. 3d) with an average particle size of 39 nm at a number content of 99.9% (Fig. 3c). The second peak contained 99.9% of particles whose average size was outside the nanorange (19500 nm), but with a number content of 0.1%.

When studying nanosystem 3, the peak of the number distribution of particles fell on 72 nm (Fig. 3e). Their amount in the liquid was 99.9%, and the volume fraction was 0.1%. In the volume distribution, the peak with a maximum at 21600 nm (Fig. 3f) gave 99.9% of particles with a number of 0.1%.

Two fractions of particles were determined in nanosystem 4. The first fraction contained NPs with a maximum of 65 nm (Fig. 3g). Their number share exceeded 99.9%, and the volume share was 0.1%. Larger particles (the second fraction) in the liquid had an average diameter of about 7100 nm (Fig. 3h). These large particles predominated by volume (about 99.9%), but their number was less than 0.1%.

Thus, DLS studies confirmed the presence of particles in the nanoscale range in all investigated nanosystems 1-4.

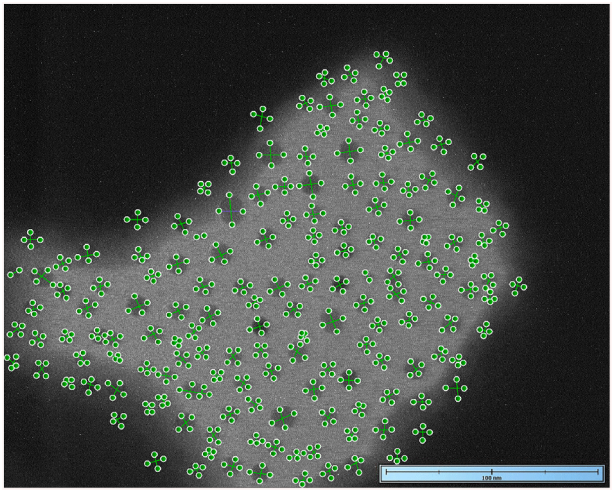

Fig. 2. TEM images of the 29 wt% Fe-NaCl condensates after rinsed in distilled water from salt.

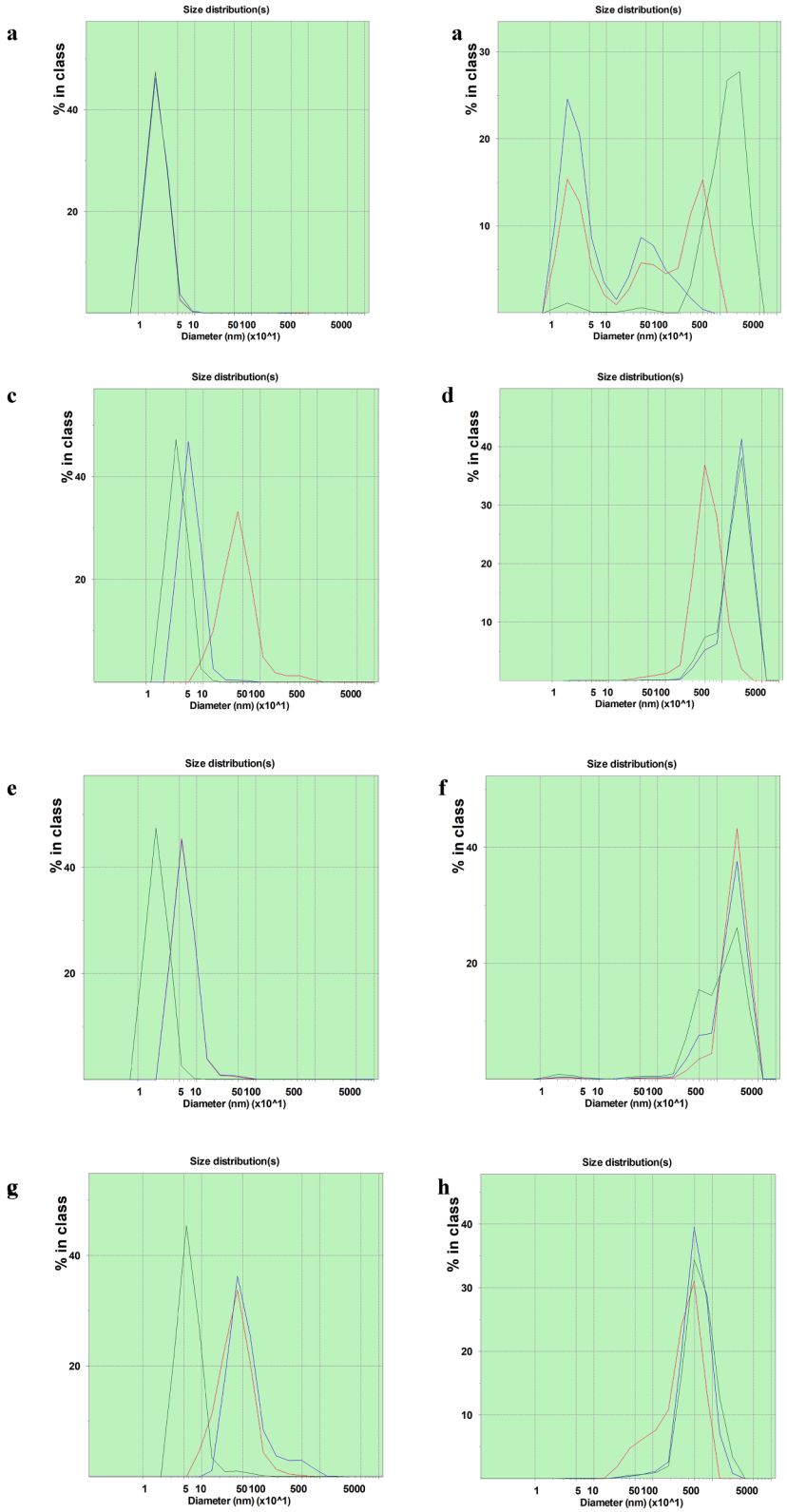

Fig. 3. Number (**a, c, e, g**) and volume (**b, d, f, h**) size distribution of magnetite particles in nanosystems 1 (**a, b**), 2 (**c, d**), 3 (**e, f**), 4 (**g, h**) in Contin approximations for three consecutive measurements (red, blue, green).

3.3. Nanoparticles effect on the pathology of erythrocyte shape

In suspensions of erythrocytes, prepared in a 0.9% buffered solution of NaCl, all types of the erythrocyte shape pathology with a prevalence of acanthocytes were detected (Table 1). This may be associated with the damage of a part of erythrocytes, especially their membranes, during the preparation of model systems and their incubation.

After incubation of erythrocyte suspensions with Fe_3O_4@NaCl NPs at concentrations of 1-100 μg Fe/ml, the total count of erythrocytes of pathological shape and the distribution of their individual types remained the same as in the control. At a concentration of 200 μg Fe/ml, Fe_3O_4@NaCl NPs increased the content of acanthocytes in the suspension by 1.5 times ($p<0.05$), the number of ovalocytes by 2.2 times ($p<0.01$) and spherocytes by 2.3 times ($p<0.05$) compared to the control. The total number of pathological forms of red blood cells increased in this group by 1.6 times ($p<0.05$).

Under the same conditions, Fe_3O_4@NaCl@EMHPS in none of the used concentrations had any effect on individual types of damaged erythrocytes and the total number of their pathological forms compared to the control (Table 2).

A similar picture occurred when Fe_3O_4@NaCl@PVP NPs were added to the erythrocyte suspensions at the concentrations of 1-100 μg Fe/ml (Table 3).

In this series of experiments, the introduction of NPs with NaCl and PVP into the erythrocyte suspension up to 200 μg Fe/ml caused an increase in the total count of pathological forms by 1.4 times ($p<0.05$) compared to the control. An increase in the content of acanthocytes by 1.4 times ($p<0.05$), ovalocytes by 2.5 times ($p<0.05$) and a tendency to an increase of the number of spherocytes ($p<0.1$) was observed.

Fe_3O_4@NaCl@PVP@EMHPS in none of the used concentrations had any effect on individual types of damaged erythrocytes and the total count of their pathological forms compared to the control (Table 4), which was similar to the effects of nanosystem 2 (Fe_3O_4@NaCl@EMHPS).

3.4. Effect of nanosystems 1-4 on hemolysis of erythrocytes

It was established that in all samples, a probable increase in hemolysis was observed only at high concentration of NPs (Fig. 4). At a concentration of up to 100 μg Fe/ml, NPs did not change hemolysis level compared to the control.

When erythrocytes were incubated with NPs of magnetite with NaCl coating at a concentration of 100 μgFe/ml, hemolysis increased on average to 3.3% versus 1.8% in the control ($p<0.1$), and at a concentration of 200 μg Fe/ml, this parameter elevated on average to 4.4% ($p<0.005$). When erythrocytes were incubated with Fe_3O_4@NaCl@EMHPS, at a concentration of 200 μg Fe/ml, hemolysis increased to 3.6% ($p<0.05$). When applying PVP-modified magnetite-NaCl NPs at a concentration of 100 μg Fe/ml, there was a tendency to the increase of hemolysis up to 3.2% ($p<0.1$), and at a concentration of 200 μg Fe/ml - its probable enhance to 5.1% ($p<0.001$) compared to the control. Fe_3O_4@NaCl@PVP@ caused a tendency to the increase of hemolysis up to 2.8% ($p<0.25$) at 100 μg Fe/ml or its significant increase up to 3.4% ($p<0.05$) at 200 μg Fe/ml. Nanosystems 2 and 4 with an antioxidant EMHPS in the maximum concentration 1.2-1.3 times less damaged erythrocytes compared to nanosystem 1, containing Fe_3O_4@NaCl NPs ($p<0.25$ and $p<0.05$, respectively). A similar relationship was observed when comparing with the effect of nanosystem 3.

Therefore, magnetite NPs functionalized with NaCl, EMHPS, and PVP caused not only an increase in the count of pathological forms of erythrocytes, but also hemolysis only at a concentration greater than 100 μg Fe/ml, and the presence of EMHPS in the nanosystem reduced these processes.

3.5. Expression of phosphatidylserine on erythrocytes under the action of nanoparticles

The expression of phosphatidylserine located on the outer surface of the membrane was quantified using flow cytometry when erythrocytes were exposed to the nanosystems at 100 μg Fe/ml. Examples of the received graphic images of cells distribution in samples of the each group are presented in Fig. 5.

The content of erythrocytes expressing phosphatidylserine on the outer surface of the cell membrane was 0.037±0.005% after incubation of these cells in an isotonic medium without NPs (control) (Fig. 5a and b). When Fe_3O_4@NaCl NPs were added to the samples, the number of cells expressing phosphatidylserine after 24 h of incubation was equal to 0.05±0.001% and exceeded the

Table 1
The content of erythrocytes with pathological shape in model systems under the action of magnetite nanoparticles with NaCl coating (M±m), per mill.

Used agent	Acanthocytes	Ovalocytes	Spherocytes	Target cells	Total amount
Control, n=5	231±36	11.4±3.8	7.0±3.6	4.2±1.3	254±47
Fe_3O_4@NaCl, 1 μg Fe/ml, n=5	229 ±15	7.2±0.9	2.8±1.6	5.8±1.7	245±23
Fe_3O_4@NaCl, 5 μg Fe/ml, n=5	223±34	8.8±5.4	4.2±2.1	6.8±1.6	243±37
Fe_3O_4@NaCl, 10 μg Fe/ml, n=5	227±26	5.4±2.2	4.8±0.8	2.2 ± 0.5	239±31
Fe_3O_4@NaCl, 100 μg Fe/ml, n=5	264±43	16.4±1.9	8.4 ± 1.7	9.2±4.3	298±48
Fe_3O_4@NaCl, 200 μg Fe/ml, n=5	351±17*	25.6±2.4*	16.4±3.4*	6.0 ±1.4	399±40*

Footnotes: In Tables 1-4:
1. n - number of observations.
2. The content of normocytes is not given; it is equal to 1000 minus the total number of pathological forms.
3. * – $p<0.05$ as compared to control.

Table 2
The content of erythrocytes with pathological shape in model systems under the action of magnetite nanoparticles with NaCl coating, additionally functionalized with ethylmethylhydroxypyridine succinate (M±m), per mill.

Used agent	Acanthocytes	Ovalocytes	Spherocytes	Target cells	Total amount
Control, n=5	257±31	6.4±1.7	8.6±2.3	11.6±1.7	284±13
Fe_3O_4@NaCl@ EMHPS, 1 μg Fe/ml, n=5	227±35	6.2±2.6	6.4±1.3	8.8±1.7	247±38
Fe_3O_4@NaCl@ EMHPS, 5 μg Fe/ml, n=5	232±20	8.2±3.7	4.8±2.3	7.8 ± 2.7	253±21
Fe_3O_4@NaCl@ EMHPS, 10 μg Fe/ml, n=5	234±14	10.4±3.7	3.8±1.8	6.6 ± 3.5	255±17
Fe_3O_4@NaCl@ EMHPS, 100 μg Fe/ml, n=5	286±32	9.6±3.5	4.6±1.7	4.2 ± 2.4	304±35
Fe_3O_4@NaCl@ EMHPS, 200 μg Fe/ml, n=5	313±19	11.8±3.5	2.4 ± 1.1	8.4 ± 2.4	336±32

Table 3
The content of erythrocytes with pathological shape in model systems under the action of magnetite nanoparticles with NaCl coating additionally functionalized with PVP (M±m), per mill.

Used agent	Acanthocytes	Ovalocytes	Spherocytes	Target cells	Total amount
Control, n=5	248±30	9.0±2.5	14.8±4.8	11.0±1.8	283±30
Fe_3O_4@NaCl@PVP, 1 μg Fe/ml, n=5	254±43	9.4±1.4	9.0±1.4	13.0±1.5	285±46
Fe_3O_4@NaCl@PVP, 5 μg Fe/ml, n=5	232±24	11.6±3.5	8.6±2.4	10.2±2.6	262±23
Fe_3O_4@NaCl@PVP, 10 μg Fe/ml, n=5	250±21	12.4±3.6	8.8±3.2	10.0±2.4	281±24
Fe_3O_4@NaCl@PVP, 100 μg Fe/ml, n=5	277±18	19.0 ±5.4	13.0±1.4	16.6±1.9	326±33
Fe_3O_4@NaCl@PVP, 200 μg Fe/ml, n=5	338±25*	26.4±4.8*	23.2±2.9	14.1±1.8	402±42*

Table 4
The content of erythrocytes with pathological shape in model systems under the action of magnetite nanoparticles with NaCl coating, additionally functionalized with ethylmethylhydroxypyridine succinate and PVP (M±m), per mill.

Used agent	Acanthocytes	Ovalocytes	Spherocytes	Target cells	Total amount
Control, n=5	267±31	5.4±1.7	7.6±2.3	8.6±1.7	289±13
Fe_3O_4@NaCl@PVP@ EMHPS, 1 μg Fe/ml, n=5	245±35	6.2±2.6	8.4±1.3	8.8±1.7	268±28
Fe_3O_4@NaCl@PVP@ EMHPS, 5 μg Fe/ml, n=5	252±20	8.2±3.7	6.8±2.3	7.8 ± 2.7	275±21
Fe_3O_4@NaCl@PVP@ EMHPS, 10 μg Fe/ml, n=5	274±14	10.4±2.7	7.8±1.8	6.6 ± 2.5	299±27
Fe_3O_4@NaCl@PVP@ EMHPS, 100 μg Fe/ml, n=5	280±32	9.6±3.5	6.6±1.7	4.2 ± 1.4	300±35
Fe_3O_4@NaCl@PVP@ EMHPS, 200 μg Fe/ml, n=5	308±29	11.8±3.5	8.4 ± 1.9	8.4 ± 2.4	337±32

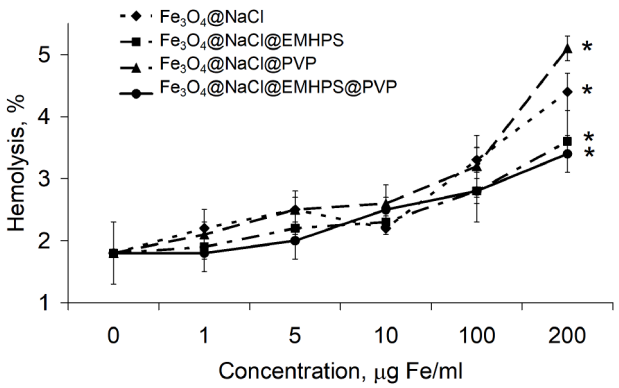

Fig. 4. Dependence of erythrocyte hemolysis on the concentration of nanoparticles in the model system. * $p<0.05$ compared to the control (erythrocyte suspension without NPs)

control probably ($p<0.05$) (Fig. 5c and d). In other model system with the addition of Fe_3O_4@NaCl@EMHPS, this parameter was 0.043 ±0.007% and did not differ from that in the control and in the previous group (Fig. 5e and f). After incubation of erythrocytes with Fe_3O_4@NaCl@PVP, the content of erythrocytes with disturbed membrane asymmetry was 0.057±0.005% (Fig. 5g and h). This is 1.5 times more compared to the control ($p<0.05$). Incubation of erythrocytes with Fe_3O_4@NaCl@PVP@EMHPS NPs produced a tendency to increase the content of cells expressing phosphatidylserine on the outer membrane ($p<0.25$) in comparison with control samples (Fig. 5i and j). It was equal to 0.047±0.003%.

Therefore, an increase in the number of erythrocytes with phosphatidylserine on the outer surface of the membrane was demonstrated by Fe_3O_4@NaCl and Fe_3O_4@NaCl@ PVP NPs at a concentration of 100 μg Fe/ml.

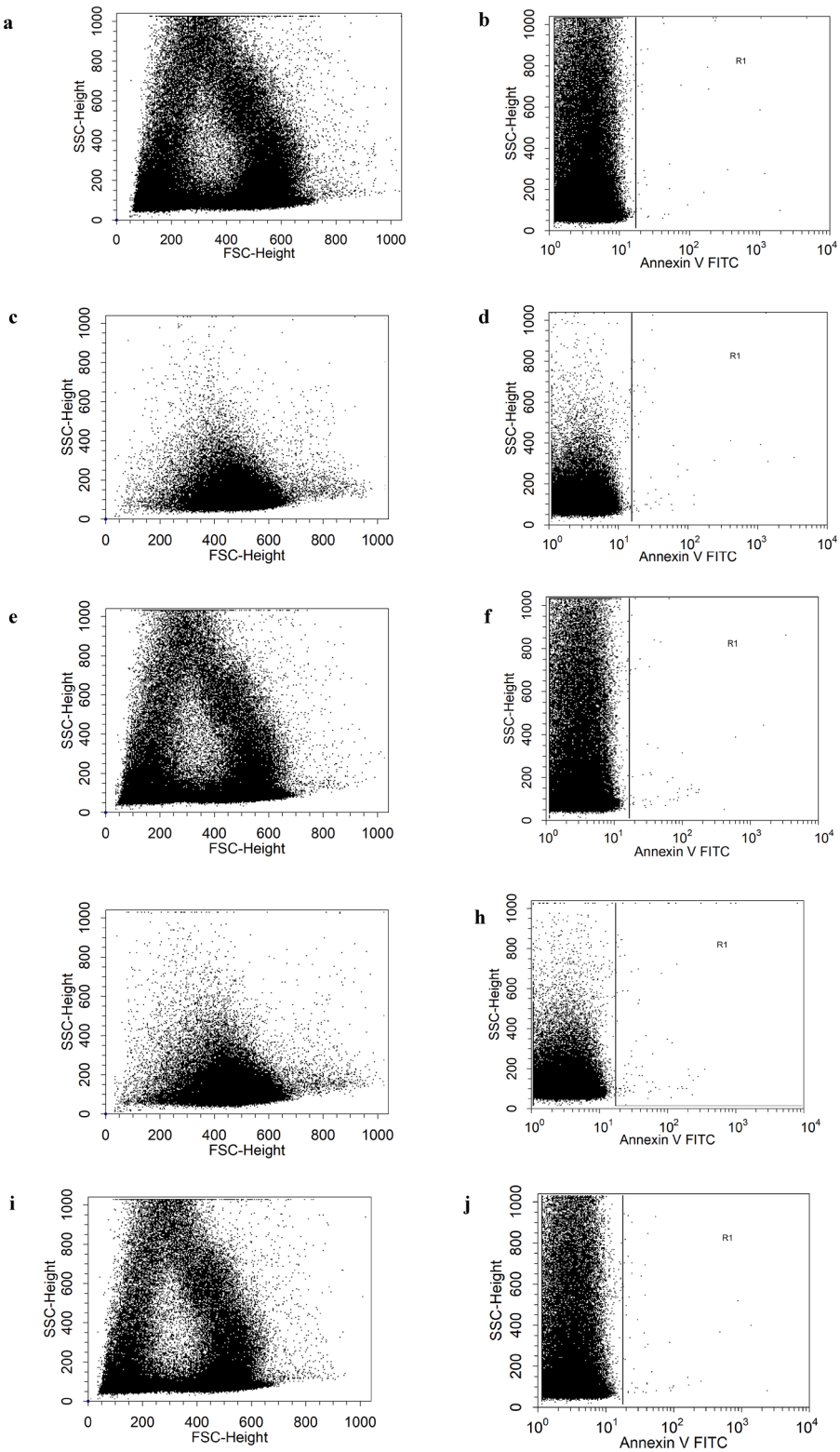

Fig. 5. Annexin V – phosphatidylserine confocal images of erythrocytes incubated with magnetite NPs at a concentration of 100μg Fe/ml (**a, c, e, g, i** - "event" distribution, **b, d, f, h, j** – annexin V cofocal images). (**a, b**) control, (**c, d**) Fe_3O_4@NaCl, (**e, f**) Fe_3O_4@NaCl@EMHPS, (**g, h**) Fe_3O_4@-NaCl@PVP, (**i, j**) Fe_3O_4@NaCl@PVP@EMHPS.

4. Discussion

The use of ligand-free methods in the synthesis of metal NPs and their oxides, to which the EB PVD method belongs, was used in the preparation of NPs for studies of cytotoxicity [47,48], antibacterial [49] or biological activity [50]. But this is poorly represented in the literature due to the labor-intensiveness and cost of the EB PVD process of NP synthesis and to the inaccessibility of the EB PVD process to most consumers. However, the need for the synthesis of pure, ligand-free NPs remains relevant, especially when used for medical and scientific purposes.

All existing methods of mass synthesis of NPs, without exception, cannot guarantee the purity of the surface of NPs. In order to unequivocally guarantee the therapeutic properties of the NP itself, it is necessary to level the effect of contamination of the NP surface. This determined the choice for the study of pure ligand-free NPs synthesized by the EB PVD method. The conducted study showed that along with the more common chemical, physicochemical and biological methods of magnetite NPs synthesis [51], the use of EB PVD technology, which provides a high yield of ligand-free metal NPs with subsequent oxidation to oxide, is fully justified [42]. In the applied version of the technology, NPs were deposited in a porous matrix of NaCl which itself is a biocompatible hydrophilic material.

Dissolving the condensate of magnetite NPs with NaCl in water created a nanosystem where there were NPs with a hydrodynamic diameter greater than that determined in solid samples washed from salt (Fig. 2). This may be due to the coating and/or formation of aggregates due to Van der Waals forces. This assumption is supported by the fact that the use of surface-active substances in the solution of NPs deposited by electron beam technology or heating allowed breaking the aggregates to a certain extent and approaching the actual size of NPs determined by TEM [42,52].

We have demonstrated that magnetite NPs with NaCl can be functionalized with a polymer (PVP) and an organic substance (EMHPS) or both of these agents. The size distribution of NPs in solutions of Fe_3O_4@NaCl@PVP (nanosystem 3) and Fe_3O_4@-NaCl@PVP@EMHPS (nanosystem 4) was characterized by a significant number of NPs up to 100 nm, which, together with coating by pharmaceuticals, created prospects for their application in medicine and required research safety and biocompatibility, in particular with blood cells.

In most cases, the assessment of hemocompatibility of NPs is based on hemolysis analysis [53], which is not sensitive enough to reflect the full range of erythrocyte damage. Therefore, we chose the approach recommended by [36], which takes into account both changes in the structure of the cell membrane and the level of hemolysis.

Our data demonstrated that a safe and non-cytotoxic concentration of NPs is up to 100 μg Fe/ml, which is consistent with literature data. Only when the concentration of NPs increased to 200 μg Fe/ml, the level of hemolysis after the incubation of nanosystems 1-4 increased, but this increase was not dramatic and did not reach 5.5%. Knowing the chemical composition of Fe_3O_4@NaCl condensate, it was possible to calculate that 100-200 μg Fe/ml, at which erythrocyte damage begins, corresponds to the NPs concentration 345-690 μg/ml. This is consistent, for example, with the work, where the cytotoxicity of uncoated magnetite NPs or NPs coated with amino acids up to a concentration of 373 μg/ml was absent [54].

However, our data showed that the increase in the number of cells with the externalization of phosphatidylserine on the outer monolayer caused by two types of functionalized magnetite NPs (Fe_3O_4@NaCl and Fe_3O_4@NaCl@PVP) was detected already at 100 μg Fe/ml. This was consistent with the opinion of other authors that assessment of externalization is more sensitive than testing for hemolysis [55,56] or the content of pathological forms of erythrocytes determined by the light microscopy, the probable changes of which were registered at twice more concentration. It should also be noted that acanthocytes, the cells with membrane damage, predominated among erythrocytes of the abnormal shape.

The detected binding of annexin V indicates changes in the characteristics of the cell surface, organization of phospholipids and membrane integrity and can be considered as an early sign of cytotoxicity of the investigated NPs. Phosphatidylserine plays a key role in the cell cycle signaling, especially in connection with apoptosis [57], so it is logical to assume that magnetite NPs induce this process at a certain concentration. Obviously, the externalization of phosphatidylserine and the associated transformation of the erythrocyte shape will lead to increased eryptosis in the body, contribute to changes in mechanical properties and phagocytic absorption of damaged erythrocytes, which will lead to changes in hematological and hemorheological parameters after the administration of high doses of magnetite NPs and certain their functionalization.

There are reports that an increase in the intracellular reactive oxygen species can cause toxicity of NPs in erythrocytes [58], and antioxidant NPs are able to inhibit this negative effect [59]. Our results indirectly confirmed this opinion. After all, both the expression of phosphatidylserine and the pathology of the erythrocyte shape were less pronounced under the action of nanosystems 2 and 4, which included the antioxidant EMHPS. Analogical situation was also observed with a level of hemolysis at a concentration of 200 μg Fe/ml.

In the conducted experiments, there was no clear correlation between the content of pathological forms and hemolysis of erythrocytes at the same concentration of 200 Fe μg/ml, which requires to agree with the opinion that under the influence of magnetite NPs, eryptosis, characterized by the appearance of pathological changes in the cell membrane of erythrocytes, does not cause acute hemolysis and release of hemoglobin, but occurs simultaneously with it [36].

5. Conclusion

EB PVD technology makes it possible to obtain magnetite NPs that can be functionalized with various chemicals, including as pharmaceuticals. The dissolution of such functionalized NPs creates nanofluids convenient for biomedical applications. This application is related to the evaluation of the safety and biocompatibility of the obtained nanosystems. Estimates based on *in vitro* erythrocyte model reflect the risks associated with damage to these blood cells by magnetite NPs, which can be extrapolated to processes in

the circulatory system *in vivo*. All studied functionalized magnetite NPs had a low cytotoxicity and were completely hematocompatible at concentrations up to 100 μg Fe/ml. An increase in the number of erythrocytes with cell membrane asymmetry was observed for nanosystems based on magnetite, NaCl, and PVP at a lower concentration than increased hemolysis and an increase in pathological forms of erythrocytes. This study indicates that exposure to phosphatidylserine may serve as a sensitive predictor of erythrocyte damage by NPs. In all tests performed, the presence of an antioxidant in the nanosystem reduced the cytotoxicity of NPs, which may indirectly indicate the role of oxidative stress in the processes of nanotoxicity and, at the same time, allows controlling these processes by applying antioxidants to modify the surface of iron oxide NPs.

Credit statement

Lytvyn S. Investigation, Formal analysis (TEM, XRD, DLS), Visualization, Writing – review and editing
Vazhnichaya E.: Conceptualization, Data curation, Investigation (nanoparticles functionalization), Writing – original draft
Kurapov Yu.: Conceptualization, Methodology of physical experiments, Project administration
Semaka O.: Investigation, Formal analysis (hemolysis, pathology of the erythrocyte shape), Resources
Babijchuk L.: Methodology of biomedical experiments, Writing – review and editing
Zubov P.: Investigation and formal analysis (cytometry)

Permission to publish

Not required.

Funding sources

This research did not receive any specific grant from funding agencies in the public, commercial, or not-for-profit sectors.

Declaration of competing interest

On behalf of all authors, the corresponding author states that there is no conflict of interest.

References

[1] S.T. Fateh, M.A. Kamalabadi, A. Aliakbarniya, S. Jafarinejad-Farsangi, M. Koohi, E. Jafari, Z.M. Karam, F. Keyhanfar, A.S. Dezfuli, Hydrophobic@ amphiphilic hybrid nanostructure of iron-oxide and graphene quantum dot surfactant as a theranostic platform, OpenNano 6 (2022), 100037, https://doi.org/10.1016/j.onano.2022.100037.
[2] T. Niemiec, M. Dudek, N. Dziekan, S. Jaworski, A. Przewozik, E. Soszka, A. Koperkiewicz, P. Koczoń, The method of coating Fe_3O_4 with carbon nanoparticles to modify biological properties of oxide measured *in vitro*, J. AOAC Internati. 100 (4) (2017) 905–915, https://doi.org/10.5740/jaoacint.17-0165.
[3] C. Martinez-Boubeta, K. Simeonidis, J. Oró, A. Makridis, D. Serantes, L. Balcells, Finding the limits of magnetic hyperthermia on core-shell nanoparticles fabricated by physical vapor methods, Magnetochemistry 7 (4) (2021) 49, https://doi.org/10.3390/magnetochemistry7040049.
[4] TK Jain, MK Reddy, MA Morales, DL Leslie-Pelecky, V. Labhasetwar, Biodistribution, clearance, and biocompatibility of iron oxide magnetic nanoparticles in rats, Mol Pharm 5 (2) (2008) 316–327, https://doi.org/10.1021/mp7001285. Mar-Apr.
[5] L. Gu, R.H. Fang, M.J. Sailor, J.H. Park, *In vivo* clearance and toxicity of monodisperse iron oxide nanocrystals, ACS Nano 6 (2012) 4947–4954, https://doi.org/10.1021/nn300456z.
[6] V. Patsula, M. Moskvin, S. Dutz, D. Horák, Size-dependent magnetic properties of iron oxide nanoparticles, J. Phys. Chem. Solids 88 (2016) 24–30, https://doi.org/10.1016/j.jpcs.2015.09.008.
[7] Y. Song, R. Wang, R. Rong, J. Ding, J. Liu, R. Li, Z. Liu, H. Li, X. Wang, J. Zhang, J. Fang, Synthesis of well-dispersed aqueous-phase magnetite nanoparticles and their metabolism as an MRI contrast agent for the reticuloendothelial system, European Journal of Inorganic Chemistry 2011 (22) (2011) 3303–3313, https://doi.org/10.1002/ejic.201100017.
[8] M. Vert, Y. Doi, K.H. Hellwich, M. Hess, P. Hodge, P. Kubisa, M. Rinaudo, F. Schué, Terminology for biorelated polymers and applications (IUPAC Recommendations 2012), Pure and Applied Chemistry 84 (2012) 377–410, https://doi.org/10.1351/PAC-REC-10-12-04.
[9] MagForce Fighting Cancer with Nanomedicine. http://www.magforce.de/en/home.html (accessed 18 Dec 2022).
[10] Feraheme Ferumoxytol Injection. https://www.feraheme.com (accessed 18 Dec 2022).
[11] T. Alishiri, H.A. Oskooei, M.M. Heravi, Fe_3O_4 Nanoparticles as an Efficient and Magnetically Recoverable Catalyst for the Synthesis of α,β-Unsaturated Heterocyclic and Cyclic Ketones under Solvent-Free Conditions, Synth. Commun. 43 (2013) 3357–3362, https://doi.org/10.1080/00397911.2013.786089.
[12] B. Jiang, L. Lian, Y. Xing, N. Zhang, Y. Chen, P. Lu, D. Zhang, Advances of magnetic nanoparticles in environmental application: Environmental remediation and (bio)sensors as case studies, Environ. Sci. Pollut. Res. 25 (2018) 30863–30879, https://doi.org/10.1007/s11356-018-3095-7.
[13] P. Salimi, O. Norouzi, S.E.M. Pourhosseini, Two-step synthesis of nanohusk Fe_3O_4 embedded in 3D network pyrolytic marine biochar for a new generation of anode materials for Lithium-Ion batteries, J. Alloys Compd. 786 (2019) 930–937, https://doi.org/10.1016/j.jallcom.2019.02.048.
[14] N. Malhotra, J.S. Lee, R.A.D. Liman, J.M.S. Ruallo, O.B. Villaflores, T.R. Ger, C.-D. Hsiao, Potential Toxicity of Iron Oxide Magnetic Nanoparticles: A Review, Molecules 25 (14) (2020) 3159, https://doi.org/10.3390/molecules25143159.
[15] S.J. Soenen, M. De Cuyper, How to assess cytotoxicity of (iron oxide-based) nanoparticles, A technical note using cationic magnetoliposomes, Contrast Media Mol. Imaging 6 (2011) 153–164, https://doi.org/10.1002/cmmi.415.
[16] A.M. Schrand, L. Dai, J.J. Schlager, S.M. Hussain, Toxicity testing of nanomaterials, in: M. Balls, R.D. Combes, N. Bhogal (Eds.), New Technologies for Toxicity Testing, Springer, Toledo, 2012, pp. 58–75, https://doi.org/10.1007/978-1-4614-3055-1_5.
[17] C.A. Schneider, W.S. Rasband, K.W. Eliceiri, Nih image to imageJ: 25 years of image analysis, Nat. Methods. 9 (2012) 671–675, https://doi.org/10.1038/nmeth.2089.
[18] D.A. Kedziorek, N. Muja, P. Walczak, J. Ruiz-Cabello, A.A. Gilad, C.C. Jie, J.W.M. Bulte, Gene expression profiling reveals early cellular responses to intracellular magnetic labeling with superparamagnetic iron oxide nanoparticles, Magn. Reson. Med. 63 (2010) 1031–1043, https://doi.org/10.1002/mrm.22290.
[19] K. Buyukhatipoglu, A.M. Clyne, Superparamagnetic iron oxide nanoparticles change endothelial cell morphology and mechanics via reactive oxygen species formation, J. Biomed. Mater. Res. Part A 96 (2011) 186–195, https://doi.org/10.1002/jbm.a.32972.

[20] S. Naqvi, M. Samim, M. Abdin, F.J. Ahmed, A. Maitra, C. Prashant, A.K. Dinda, Concentration-dependent toxicity of iron oxide nanoparticles mediated by increased oxidative stress, Int. J. Nanomed 5 (2010) 983, https://doi.org/10.2147/IJN.S13244.

[21] S. Laurent, C. Burtea, C. Thirifays, U.O. Häfeli, M. Mahmoudi, Crucial ignored parameters on nanotoxicology: The importance of toxicity assay modifications and "cell vision, PLoS ONE 7 (2012) e29997, https://doi.org/10.1371/journal.pone.0029997.

[22] A. Kunzmann, B. Andersson, C. Vogt, N. Feliu, F. Ye, S. Gabrielsson, M.S. Toprak, T. Buerki-Thurnherr, S. Laurent, M. Vahter, H. Krug, M. Muhammed, A. Scheynius, B. Fadeel, Efficient internalization of silica-coated iron oxide nanoparticles of different sizes by primary human macrophages and dendritic cells, Toxicol. Appl. Pharm. 253 (2011) 81–93, https://doi.org/10.1016/j.taap.2011.03.011.

[23] S. Correia Carreira, L. Walker, K. Paul, M. Saunders, The toxicity, transport and uptake of nanoparticles in the *in vitro* bewo b30 placental cell barrier model used within nanotest, Nanotoxicology 9 (1) (2015) 66–78, https://doi.org/10.3109/17435390.2013.833317.

[24] Y.-R. Lin, C.-J. Kuo, H.Y.-H. Lin, C.-J. Wu, S.-S. Liang, A proteomics analysis to evaluate cytotoxicity in NRK-52e cells caused by unmodified nano-Fe_3O_4, Sci. World J. 2014 (2014), 754721, https://doi.org/10.1155/2014/754721.

[25] W. Ma, P.M. Gehret, R.E. Hoff, L.P. Kelly, W.H. Suh, The investigation into the toxic potential of iron oxide nanoparticles utilizing rat pheochromocytoma and human neural stem cells, Nanomaterials 9 (3) (2019) 453, https://doi.org/10.3390/nano9030453.

[26] M. Marcus, M. Karni, K. Baranes, I. Levy, N. Alon, S. Margel, O. Shefi, Iron oxide nanoparticles for neuronal cell applications: Uptake study and magnetic manipulations, J. Nanobiotechnol. 14 (1) (2016) 37, https://doi.org/10.1186/s12951-016-0190-0.

[27] D. Ling, T. Hyeon, Chemical design of biocompatible iron oxide nanoparticles for medical applications, Small 9 (9-10) (2013) 1450–1466, https://doi.org/10.1002/smll.201202111.

[28] U.O. Häfeli, J.S. Riffle, L. Harris-Shekhawat, A. Carmichael-Baranauskas, F. Mark, J.P. Dailey, D. Bardenstein, Cell uptake and *in vitro* toxicity of magnetic nanoparticles suitable for drug delivery, Mol. Pharm. 6 (2009) 1417–1428, https://doi.org/10.1021/mp900083m.

[29] H. Nosrati, M. Salehiabar, E. Attari, S. Davaran, H. Danafar, H.K. Manjili, Green and one-pot surface coating of iron oxide magnetic nanoparticles with natural amino acids and biocompatibility investigation, Appl. Organomet. Chem. 32 (2) (2018) e4069, https://doi.org/10.1002/aoc.4069.

[30] G. Liu, J. Gao, H. Ai, X. Chen, Applications and potential toxicity of magnetic iron oxide nanoparticles, Small 9 (2013) 1533–1545, https://doi.org/10.1002/smll.201201531.

[31] R. Mejías, L. Gutiérrez, G. Salas, S. Pérez-Yagüe, T.M. Zotes, F.J. Lázaro, M.P. Morales, Long term biotransformation and toxicity of dimercaptosuccinic acid-coated magnetic nanoparticles support their use in biomedical applications, J. Control Release. 171 (2013) 225–233, https://doi.org/10.1016/j.jconrel.2013.07.019.

[32] D. Stamopoulos, E. Manios, V. Gogola, D. Niarchos, M. Pissas, On the biocompatibility of Fe_3O_4 ferromagnetic nanoparticles with human blood cells, J. Nanosci. Nanotechnol. 10 (9) (2010) 6110–6115, https://doi.org/10.1166/jnn.2010.2616.

[33] K. Müller, J.N. Skepper, M. Posfai, R. Trivedi, S. Howarth, C. Corot, E. Lancelot, P.W. Thompson, A.P. Brown, J.H. Gillard, Effect of ultrasmall superparamagnetic iron oxide nanoparticles (ferumoxtran-10) on human monocyte-macrophages *in vitro*, Biomaterials 28 (2007) 1629–1642, https://doi.org/10.1016/j.biomaterials.2006.12.003.

[34] D.E. Creangă, M. Culea, C. Nădejde, S. Oancea, L. Curecheriu, M. Racuciu, Magnetic nanoparticle effects on the red blood cells, J. Phys.: Conf. Ser. 170 (1) (2009), 012019, https://doi.org/10.1088/1742-6596/170/1/012019.

[35] Scientific Committee on Consumer Safety. Guidance on the safety assessment of nanomaterials in cosmetics. SCCS/1611/19. Adopted 30-31 Oct, 2022. 113 p. https://health.ec.europa.eu/system/files/2020-10/sccs_o_233_0.pdf (accessed 28 Nov 2022).

[36] Q. Ran, Y. Xiang, Y. Liu, L. Xiang, F. Li, X. Deng, Y. Xiao, L. Chen, L. Chen, Z. Li, Eryptosis Indices as a Novel Predictive Parameter for Biocompatibility of Fe_3O_4 Magnetic Nanoparticles on Erythrocytes, Sci. Rep 5 (2015) 16209, https://doi.org/10.1038/srep16209.

[37] Compendium. Mexidol (Mexidolum*). Description of the active substance. https://compendium.com.ua/akt/77/523/mexidolum/(accessed 7 Nov 2022).

[38] S.H. Burchinskyi, Comprehensive correction of anxiety and cognitive disorders in angioneurology: goals, objectives, tools, International neurological journal 94 (2017) 73–78, https://doi.org/10.22141/2224-0713.8.94.2017.120704.

[39] Compendium Medicines. Neohaemodez (Neohaemodesum). https://compendium.com.ua/dec/262116/(accessed 17 Nov 2022).

[40] V. Llaneza, I. Rodea-Palomares, Z. Zhou, R. Rosal, F. Fernández-Pina, J.C.J. Bonzongo, Polyvinylpyrrolidone and arsenic-induced changes in biological responses of model aquatic organisms exposed to iron-based nanoparticles, Journal of Nanoparticle Research 18 (2016) 1–12, https://doi.org/10.1007/s11051-016-3541-8.

[41] L. Wang, C. Shen, Y. Cao, PVP modified Fe_3O_4@SiO_2 nanoparticles as a new adsorbent for hydrophobic substances, Journal of Physics and Chemistry of Solids 133 (2019) 28–34, https://doi.org/10.1016/j.jpcs.2019.05.004.

[42] Yu.A. Kurapov, S.E. Litvin, S.M. Romanenko, G.G. Didikin, E.I. Oranskaya, Controllable synthesis of iron oxide nanoparticles in porous NaCl matrix, Materials Research Express 4 (3) (2017), 035031, https://doi.org/10.1088/2053-1591/4/3/035031.

[43] H.G. Merkus, Particle size measurements: Fundamentals, practice, quality, Springer, Dordrecht, 2009. https://link.springer.com/book/10.1007/978-1-4020-9016-5.

[44] S. Parasuraman, R. Raveendran, R. Kesavan, Blood sample collection in small laboratory animals, J. Pharmacol. Parmacother. 1 (2) (2010) 87–93, https://doi.org/10.4103/0976-500X.72350.

[45] A.S. Adewoyin, O. Adeyemi, N.O. Davies, A.A. Ogbenna, Erythrocyte Morphology and Its Disorders, in: A. Tombak (Ed.), Erythrocyte, IntechOpen, London, 2019, https://doi.org/10.5772/intechopen.86112. https://www.intechopen.com/chapters/67667 (accessed 05 Dec 2022).

[46] F.A. Kuypers, R.A. Lewis, M. Hua, M.A. Schott, D. Discher, J.D. Ernst, B.H. Lubin, Detection of altered membrane phospholipid asymmetry in subpopulations of human red blood cells using fluorescently labeled annexin V, Blood 87 (3) (1996) 1179–1187, https://doi.org/10.1182/blood.V87.3.1179.bloodjournal8731179.

[47] U. Taylor, C. Rehbock, C. Streich, D. Rath, S. Barcikowski, Rational design of gold nanoparticle toxicology assays: a question of exposure scenario, dose and experimental setup, Nanomedicine 9 (2014) 1971–1989, https://doi.org/10.2217/nnm.14.139.

[48] A.I. Becerro, D. González-Mancebo, E. Cantelar, F. Cussó, G. Stepien, J.M. de la Fuente, M. Ocana, Ligand-free synthesis of tunable size Ln: BaGdF5 (Ln= Eu3+ and Nd3+) nanoparticles: luminescence, magnetic properties, and biocompatibility, Langmuir 32 (2016) 411–420, https://doi.org/10.1021/acs.langmuir.5b03837.

[49] X. Zhang, Y. Li, X. Luo, Y. Ding, Enhancing antibacterial property of porous titanium surfaces with silver nanoparticles coatings via electron-beam evaporation, Journal of Materials Science: Materials in Medicine 33 (2022) 1–11, https://doi.org/10.1007/s10856-022-06679-y.

[50] S.Ye. Lytvyn, Yu.A. Kurapov, N.M. Ruban, L.N. Churkina, I.M. Andrusyshyna, G.G. Didikin, V.V. Boretskyi, Influence of temperature on the physical properties and bio-activity of pure (ligand-free) EB PVD silver nanoparticles, Applied Nanoscience 2022, Published 26 December 2022. 10.1007/s13204-022-02730-0.

[51] A. Ali, H. Zafar, M. Zia, I. Ul Haq, A.R. Phull, J.S. Ali, A. Hussain, Synthesis, characterization, applications, and challenges of iron oxide nanoparticles, Nanotechnol. Sci. Appl. 9 (2016) 49–67, https://doi.org/10.2147/NSA.S99986.

[52] Yu.A. Kurapov, S.Ye. Lytvyn, G.G. Didikin, S.M. Romanenko, Electron-Beam Physical Vapor Deposition of Iron Nanoparticles and Their Thermal Stability in the Fe-O System, Powder Metallurgy and Metal Ceramics 60 (2021) 451–463, https://doi.org/10.1007/s11106-021-00256-8.

[53] K.M. de la Harpe, P.P.D. Kondiah, Y.E. Choonara, T. Marimuthu, L.C. du Toit, V. Pillay, The Hemocompatibility of Nanoparticles: A Review of Cell-Nanoparticle Interactions and Hemostasis, Cells 8 (2019) 1209, https://doi.org/10.3390/cells8101209.

[54] H. Nosrati, M. Salehiabar, E. Attari, S. Davaran, H. Danafar, H.K. Manjili, Green and one-pot surface coating of iron oxide magnetic nanoparticles with natural amino acids and biocompatibility investigation, Appl. Organomet. Chem. 32 (2018) e4069, https://doi.org/10.1002/aoc.4069.

[55] A. Lupescu, K. Jilani, C. Zelenak, M. Zbidah, S.M. Qadri, F. Lang, Hexavalent chromium-induced erythrocyte membrane phospholipid asymmetry, Biometals 25 (2012) 309–318, https://doi.org/10.1007/s10534-011-9507-5.

[56] K. Jilani, F. Lang, Ca^{2+}-dependent suicidal erythrocyte death following zearalenone exposure, Arch. Toxicol. 87 (2013) 1821–1828, https://doi.org/10.1007/s00204-013-1037-1.

[57] M.C. Wesseling, L. Wagner-Britz, H. Huppert, B. Hanf, L. Hertz, D.B. Nguyen, I. Bernhardt, Phosphatidylserine Exposure in Human Red Blood Cells Depending on Cell Age, Cell Physiol. Biochem. 38 (2016) 1376–1390, https://doi.org/10.1159/000443081.
[58] A. Nemmar, S. Beegam, P. Yuvaraju, J. Yasin, A. Shahin, B.H. Ali, Interaction of amorphous silica nanoparticles with erythrocytes *in vitro*: role of oxidative stress, Cell Physiol. Biochem. 34 (2014) 255–265, https://doi.org/10.1159/000362996.
[59] D.B. Cochran, P.P. Wattamwar, R. Wydra, J.Z. Hilt, K.W. Anderson, R.E. Eitel, T.D. Dziubla, Suppressing iron oxide nanoparticle toxicity by vascular targeted antioxidant polymer nanoparticles, Biomaterials 34 (2013) 9615–9922, https://doi.org/10.1016/j.biomaterials.2013.08.025.